Journal of Medicinal Chemistry

Article

Development of 5-aminopyrazole-4-carboxamide-based bumped-kinase inhibitors for Cryptosporidiosis therapy

Wenlin Huang, Matthew A. Hulverson, Ryan Choi, Samuel L.M. Arnold, zhongsheng zhang, Molly McCloskey, Grant Whitman, Robert Hackman, Kasey Rivas, Lynn K Barrett, Kayode Ojo, Wesley C. Van Voorhis, and Erkang Fan

J. Med. Chem., **Just Accepted Manuscript** • DOI: 10.1021/acs.jmedchem.9b00069 • Publication Date (Web): 04 Mar 2019

Just Accepted

ACS Publications

is published by the American Chemical Society. 1155 Sixteenth Street N.W., Washington, DC 20036

Development of 5-aminopyrazole-4-carboxamide-based bumped-kinase inhibitors for Cryptosporidiosis therapy

Wenlin Huang[a], Matthew A. Hulverson[b], Ryan Choi[b], Samuel L.M. Arnold[b], Zhongsheng Zhang[a], Molly C. McCloskey[b], Grant R. Whitman[b], Robert C. Hackman[c,d,e], Kasey L. Rivas[b], Lynn K. Barrett[b], Kayode K. Ojo[b], Wesley C. Van Voorhis[b*], Erkang Fan[a*]

[a] Department of Biochemistry, University of Washington, Seattle, Washington 98195, United States
[b] Department of Medicine, Division of Allergy & Infectious Disease, Center for Emerging & Re-emerging Infectious Disease (CERID), University of Washington, Seattle, Washington 98109, United States
[c] Fred Hutchinson Cancer Research Center, Seattle, Washington 98109, United States
[d] Department of Pathology, University of Washington, Seattle, Washington 98195, United States
e Department of Laboratory Medicine, University of Washington, Seattle, Washington 98195, United States

* Corresponding authors:

Wesley C. Van Voorhis; E-mail: wesley@uw.edu

Erkang Fan; E-mail: erkang@uw.edu

ABSTRACT

Cryptosporidium is a leading cause of pediatric diarrhea worldwide. Currently there is neither a vaccine nor a consistently effective drug available for this disease. Selective 5-aminopyrazole-4-carboxamide-based bumped-kinase inhibitors (BKIs) are effective in both in vitro and in vivo models of *Cryptosporidium parvum*. Potential cardiotoxicity in some BKIs led to the continued exploration of the 5-aminopyrazole-4-carboxamide scaffold to find safe and effective drug candidates for *Cryptosporidium*. A series of newly designed BKIs were tested for efficacy against *C. parvum* using in vitro and in vivo (mouse infection model) assays, and safety issues. Compound **6** (BKI 1708) was found to be efficacious at 8 mg/kg dosed once daily (QD) for 5 days with no observable signs of toxicity up to 200 mg/kg dosed QD for 7 days. Compound **15** (BKI 1770) was found to be efficacious at 30 mg/kg dosed twice daily (BID) for 5 days with no observable signs of toxicity up to 300 mg/kg dosed QD for 7 days. Compounds **6** and **15** are

promising pre-clinical leads for cryptosporidiosis therapy with acceptable safety parameters and efficacy in the mouse model of cryptosporidiosis.

INTRODUCTION

Cryptosporidiosis, caused by the apicomplexan parasite *Cryptosporidium*, is a major contributor to global diarrheal morbidity and mortality, particularly in 6-24 month old malnourished children, and is associated with growth stunting and developmental deficits in children.[1-3] In immunocompromised individuals, *Cryptosporidium* infection becomes persistent and life threatening. Nitazoxanide, the only U.S. Food and Drug Administration-approved drug for the treatment of cryptosporidiosis, has limited efficacy in immunocompromised patients and malnourished children, and is only approved for use in children ≥1 year-old, leaving the most vulnerable patient populations without effective treatment.[4-6] Thus, new therapies with established safety and efficacy in malnourished infants and immunocompromised individuals are urgently needed for cryptosporidiosis.

Previous studies have shown that inhibition of apicomplexan calcium-dependent protein kinases interfere with the parasites' ability to invade or egress mammalian host cells.[7-9] The calcium-dependent protein kinase 1 of *C. parvum* (*Cp*CDPK1) is a promising target for drug development for cryptosporidiosis.[10-12] A recent scientific report demonstrated that knocking down *Cp*CDPK1 with small interfering RNAs (siRNAs) significantly decreased parasite invasion and growth.[12] Moreover, there was an additive effect of *Cp*CDPK1 knockdown in combination with treatment of BKIs 1294 and 1517 in reducing the proliferation of *C. parvum* parasites.[12] These results suggest that *Cp*CDPK1 is a target of BKIs.

BKIs have been developed to selectively target *Cp*CDPK1, prevent the growth of *C. parvum* in vitro and in vivo, and have proven anti-*Cryptosporidium* efficacy in the SCID/beige

immunocompromised mouse and the newborn calf *C. parvum* clinical models (Fig. 1). Pyrazolopyrimidine (PP) based BKIs 1294 and 1369 exhibited anti-*Cryptosporidium* efficacy in mouse and the newborn calf *C. parvum* clinical models.[11,13,14] Pyrrolopyrimidine (PrP) based BKIs are distinct therapeutic alternatives of PP inhibitors. PrP BKI 1649 potently inhibited *Cp*CDPK1, prevented the growth and proliferation of *C. parvum* in vitro, and reduced oocyst shedding in a mouse model of cryptosporidiosis.[15] 5-aminopyrazole-4-carboxamide (AC) scaffold BKIs are also potent inhibitors of *C. parvum* growth in vitro[16, 17] and in the SCID/beige immunocompromised mouse and the newborn calf *C. parvum* clinical models.[12, 13]

Despite their promising efficacies, some BKIs have shown toxicity issues that limit their potential for human treatment. PP BKI 1294 has shown activity against the human ether-á-go-go related gene (hERG) in vitro.[18] While AC BKI 1517 did not have significant in vitro hERG inhibition signal,[19] it exhibits other indicator of potential cardiac toxicity, namely a significant change in mean arterial pressure, when dosed in rats (data not shown). However, changes to the R groups in the PP scaffold has been previously shown to decrease these cardiovascular issues when compared to BKI 1294, leaving open the possibility of similarly eliminating such issues in the AC scaffold.[20] The study presented here describes the iterative improvements for efficacy and safety of the AC scaffold inhibitors which have resulted in preclinical leads, compounds **6** and **15** (BKIs 1708 and 1770, respectively) for cryptosporidiosis therapy. Compounds **6** and **15** potently inhibit activity of *Cp*CDPK1 and reduce oocyst shedding in *C. parvum* infected interferon-γ knock out (IFN-γ KO) mice. In addition, both **6** and **15** are safe in that they lack mutagenic activity, are not toxic to a variety of human cell lines, show substantial improvement over BKI 1294 in hERG assays, and can be administered orally to mice up to 200 to 300 mg/kg of body weight for 7 days with little to no signs of toxicity.

RESULTS AND DISCUSSION

Molecular design and synthesis

We previously developed a number of highly promising AC scaffold BKIs that potently block the enzymatic activity of *Toxoplasma gondii* calcium-dependent protein kinase 1 (*Tg*CDPK1), thereby blocking the invasion of *T. gondii* into host cells.[17,20] Many of these selective inhibitors are also effective in both in vitro and in vivo models of cryptosporidiosis, especially the previously reported BKI 1517.[12,13,16] Unfortunately, BKI 1517 was found to have cardiotoxicity in rats at doses very close to therapeutic doses for cryptosporidium efficacy (data not shown).

Recent studies on the PP BKIs suggest that higher fecal levels of this BKI series may be a good proxy for elevated intraepithelial concentrations in the gastrointestinal (GI) tract and in vivo efficacy.[22] We also found that compound **7** (BKI 1608), bearing a hydroxyl aliphatic chain at the N1 position, reduced systemic exposure, high fecal levels, and in vivo efficacy in neonatal mice.[16] Thus, we investigated a series of AC BKIs with a hydroxyl aliphatic chain at the N1 position and a fixed C3 position Ar group as ethoxy or cyclopropoxy substituted quinolone/naphthyl to identify *Cp*CDPK1 inhibitors that possess distinct physiochemical properties, favorable anti-parasitic activity, and improved safety properties.

The synthesis of these AC BKIs followed previously reported procedures.[16,17,20] As shown in Scheme 1, a quinoline/naphthyl aldehyde with varied substitutions, was reacted with a hydrazine in ethanol to give the hydrazone, which was then brominated by NBS. The intermediate was then reacted with cyanoacetamide anion that was generated in situ to afford the final product. The majority of the synthetic effort was spent on generating quinoline/naphthyl aldehydes and hydrazines with desired substitutions. The synthesis of these key intermediates are reported in supporting information.

Scheme 1.

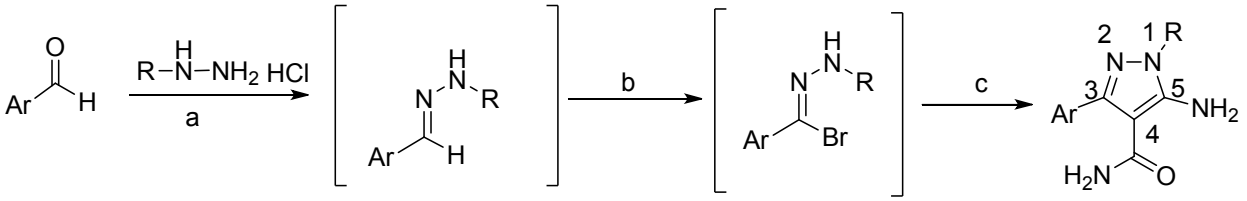

Reagents and conditions (a) DIPEA, EtOH, microwave, 70°C, 20 min; (b) NBS, DMF, 0°C, 20 min; (c) cyanoacetamide, NaH, DMF, room temperature (r.t.), overnight.

In vitro compound screening

Multiple assays were used to determine the activity and selectivity of each compound, **1-24**, with various Ar and R group constituents and variations on the position of the nitrogen within the quinoline group as compared to the naphthalene equivalents. Compounds were first tested for activity against *Cp*CDPK1 (Table 1). We were expecting all of the compounds to be potent inhibitors of *Cp*CDPK1 based on the SAR we found previously, as all the compounds bear an Ar group as ethoxy or cyclopropoxy substituted quinolone/naphthyl which are optimal substitutions.[16, 17, 20] The various hydroxyl containing R groups were also expected to be well tolerated as this functional group projects into the ribose binding pocket and the solvent.[16] Indeed, all of the compounds potently inhibit *Cp*CDPK1 at < 0.01 μM. The result is consistent with the SAR we found previously.[16] BKIs that successfully blocked in vitro activity to *Cp*CDPK1 were tested against mammalian tyrosine kinase Src (c-Src), a representative mammalian kinase, to eliminate compounds with potential off-target activities (Table 1). All compounds were then tested against Nanoluciferase expressing (Nluc) *C. parvum* infected HCT-8 cells for in vitro cellular potency and CRL-8155 and HepG2 mammalian cells for general off-target activity and toxicity (Table 1). Cellular inhibition of *C. parvum* was consistently <1 μM for most compounds (22 out of the 27 total), regardless of R groups or the quinoline/naphthyl variation.

Due to the previous prevalence of human hERG activity and its associated cardiovascular issues in BKIs of the PP scaffold,[18] compounds that displayed sufficiently promising in vitro potencies against *Cp*CDPK1 and *C. parvum* cells and lacked off-target activities against c-Src and mammalian cells were tested to determine their hERG IC_{50}s in either the thallium-based or Qpatch assays (Table 1). Additional in vitro screens were conducted to determine compound properties that may best correlate to future in vivo efficacy. These included plasma protein binding in both mouse and human plasma using dialysis membranes, and solubility at pH values present in the GI tract (2.0 and 6.5) (Table 1).

Pharmacokinetic profiling in mice

A subset of compounds were tested to determine plasma exposure and fecal concentrations after a single 10 or 25 mg/kg body weight oral dose (PO). Pharmacokinetic (PK) calculations were performed to determine maximum concentration (C_{max}), area under the curve (AUC), terminal half-life (t½), and oral clearance (Table 2). Compound excreted in feces over a 24-hour period post 25 mg/kg PO dose were also measured (Table 2). None of the PK parameters correlated with quinoline/naphthyl variants within the scaffold. There was no association between solubility and the observed C_{max} or AUC among the compounds, regardless of R groups or quinoline/naphthyl variants. In addition, solubility did not correlate with fecal levels observed after oral dosing.

Efficacy in IFN-γ KO mouse model of *C. parvum* infection

A subset of 11 compounds, **3**, **5**, **6**, **7**, **9**, **12**, **15**, **20**, **21**, **23**, and **24**, were selected for oral dosing in IFN-γ KO mice infected with Nluc expressing *C. parvum* (Table 3). Since most compounds were potent against both the *Cp*CDPK1 enzyme and *C. parvum* in vitro, these compounds were selected to represent a variety of properties, including varying solubility,

systemic exposures, fecal exposures, and half-lives, across the different groups of quinoline/naphthyl variants and the different R groups, in order to best determine which chemical properties from Tables 1 or 2 would best predict efficacy within this mouse model for the AC BKIs. Mice were dosed orally for 5 days with a dose based partially upon observed PK (Table 2). Based on the observed PK of compound **15** and previous results with twice daily (BID) dosing of AC compound 1517**,** the compound was dosed BID for the efficacy studies.[12] All other compounds were dosed once daily. Compounds **5**, **6**, **7**, **9**, **11**, **15**, **20**, **23**, and **24** all showed significant reduction in oocyst shedding at various doses (Table 3). Compounds **3** and **21** failed to reduce infection despite having a relatively high fecal concentration, suggesting a differential attribute profile requirement for in vivo efficacy of the AC relative to the PP scaffold BKIs.[20] It could also mean that some AC compounds in feces may not be associated with solubilized compound in the gastrointestinal tract.[20, 22] The efficacious compounds showed wide variations in C_{max}, AUC, t½, and fecal concentration from their respective single dose oral mouse PKs (Table 2). There was no observed correlation between efficacy and any of these PK parameters. While all compounds efficacious in mice had solubilities >50 μM at both pH 2.0 and 6.5, compounds **3** and **21** had poor solubility at least at one pH level and failed to be efficacious in the IFN-γ KO mouse model despite reasonable plasma exposure for **21** (Tables 1 and 2). These results strongly suggest a certain threshold of solubility may be required for in vivo efficacy for this class of compounds.

Additional compound evaluation

Based upon the above predicted importance of solubility in correlation to efficacy, three additional AC compounds, **25**, **26**, and **27**, were chosen for evaluation of in vitro and PK properties (Tables 1 and 2) and efficacy to confirm correlation to solubility. Compounds **25**, **26**, and **27** have unrelated R_1 and R_2 groups and all have the naphthyl variant in the central scaffold. All three had

low oral clearance, relatively high t½, and good systemic exposure from oral PK (Table 2). However, **25** had good solubility and low fecal exposure, while **26** and **27** showed poor solubility and high fecal exposures (Tables 1 and 2). When tested in Nluc expressing *C. parvum* infected IFN-γ KO mice, compound **25** was efficacious while **26** and **27** were not (Table 3). With the inclusion of compounds **25**, **26** and **27**, a strong correlation between efficacy, as represented by log reduction over untreated controls (Table 3), and solubility at pH 2.0 (r_{12}=0.93, P<0.0001) and pH 6.5 (r_{10}=0.95, P<0.0001) can be observed. A pH of 2.0 is representative of the stomach, where the compounds are first administered by oral gavage, while pH 6.5 is more representative of the intestine. Compounds **3** and **27** have high solubility at pH 2.0, but low solubility at pH 6.5. They should be highly solubilized in the stomach, but could be failing efficacy if they were partially precipitating into the intestinal lumen with the decreased solubility at the more neutral intestinal pH, thereby dropping the solubilized compound below concentrations that can enter infected epithelial cells of the small or large intestine at sufficient levels to inhibit growth of the parasites. Similarly, if compounds **21** and **26** were only solubilized at low levels in both the stomach and intestine, they would not reach sufficient concentrations to enter infected epithelial cells and inhibit parasite growth. However, efficient absorption of poorly soluble compounds may happen at sites away from parasite infection in the GI track, leading to reasonable or high plasma exposures (such as **21**, **26**, or **27**). This could also explain how compounds **3**, **21**, **26**, and **27** could reach high concentrations in the feces or even plasma but not show efficacy, as the majority of the compound would simply pass through the GI lumen in a precipitated state without ever reaching the site of infection within the intestinal epithelial cells. This may be one possible explanation for the lack of correlation (r_{10}=-0.33, P>0.2) seen between fecal levels and efficacy, contrary to what was previously observed with the PP scaffold of BKIs.[20] Given the previously established necessity to

have BKI exposure throughout the entire GI tract in order to effectively treat cryptosporidiosis in mice, it is clear that a threshold of solubility is required at all pHs present in the GI tract for a compound to be efficacious.[22] Future studies that further examine the relationship of AC compound solubility and exposure to parasites and infection sites within the different sections of the GI tract would certainly be warranted.

At this stage, many compounds were eliminated from further consideration for a variety of individual shortcomings that might make them unsuitable as a clinical treatment candidate. Table 4 shows the reasoning as to why individual compounds were either removed from consideration or moved to further testing.

Dose response and toxicity profiling

Based on their promising initial efficacy and in vitro testing results, compounds **6**, **9**, **15**, **20**, and **25** were tested using dose titrations in Nluc expressing *C. parvum* infected IFN-γ KO mice to determine the lowest possible efficacious dose in mice, while lowering C_{max} plasma levels to assist in alleviating possible toxicity concerns. Compound **6** was initially efficacious at 60 mg/kg dosed once daily (QD) for 5 days (Fig. 2A). Doses of 30, 15, and 8 mg/kg were also shown to be efficacious when administered QD for 5 days, with 3 to 4-log reductions in infection for each. Only the rates of decline varied among these doses, with the lowest doses taking slightly longer to reach the lower limits of detection (LLOD) for this assay. Plasma levels of **6** at the lowest efficacious dose of 8 mg/kg QD reached a C_{max} of 2.6 ± 0.7 μM after the 4th dose. Compound **9** was initially efficacious at a dose of 60 mg/kg QD for 5 days (Fig. 2B). Although **9** showed an improvement over untreated controls at 30 mg/kg BID, it unfortunately allowed infection levels in mice to remain a full log above the LLOD (Fig. 2B). The high dose concentration of **9** could prove to be a future liability as this compound contains a chiral center at the R group, which could drive

up manufacturing costs for a drug that is primarily aimed at resource-limited populations. Compound **15** was originally tested at 60 mg/kg BID for 5 days and showed a 4-log reduction to below the LLOD (Fig. 2C). Subsequent doses of 120 and 60 mg/kg QD, and 30, 15, and 5 mg/kg BID were administered for 5 days (Fig. 2C). Dose concentrations of 120 mg/kg QD and 30 mg/kg BID of **15** were also successful at significantly reducing oocyst shedding compared to untreated controls, with reductions to below the LLOD. However, 60 mg/kg QD and 15 and 5 mg/kg BID of **15** failed to provide an efficacious result (Fig. 2C). Plasma levels of **15** at the efficacious dose of 30 mg/kg BID reached a C_{max} of 0.51 ± 0.2 μM after the 7th dose. Compound **20** was efficacious to the LLOD at 60 mg/kg QD for 5 days, but failed to provide a significant reduction from initial infection levels at 10 or 20 mg/kg BID (Fig. 2D). The systemic exposure of **20** is relatively high (Table 2), so a reduced dose would also be ideal here to mitigate possible toxicity concerns. Compound **25** was efficacious at 60 mg/kg QD, and was further tested at 30 and 15 mg/kg QD for 5 days (Fig. 2E). The 30 mg/kg dose of **25** also reduced infection to below the LLOD, but the 15 mg/kg dose failed to reduce infections from their initial levels, despite showing an improvement over the untreated controls (Fig. 2E). Plasma levels of **25** at the efficacious dose of 30 mg/kg QD reached a C_{max} of 28.8 ± 8.9 μM after the 4th dose.

Various signs of toxicity in in vivo models have been previously observed with oral dosing of specific BKI analogs of the PP scaffold, including neurological,[23] gastrointestinal, or other general adverse reactions.[14] Based on the findings of low efficacious dose concentrations, compounds **6**, **15**, and **25** were moved to tolerability and toxicity testing in mice in order to determine if these efficacious AC compounds would induce any similar signs of toxicity. No adverse effects were seen during the highest concentration dosing in the mouse efficacies, so a single oral dose was given to mice at escalating dose concentrations until signs of toxicity were

observed as described.[23] Doses were started at 100 mg/kg for **6**, 150 mg/kg for **15**, and 100 mg/kg for **25**. This was increased to 200, 300, and 400 mg/kg for **6**, 200, 300, 400, and 600 mg/kg for **15**, and 150, 200, and 250 mg/kg for **25**. There were no observable signs of toxicity or distress from any of these dose concentrations for **6**, **15**, or **25**. However, escalation had to be stopped as all three compounds reached their limit of solubility in the dosing solutions at these concentrations.

For compound **6**, mice were dosed at 100 and 200 mg/kg QD for 7 days to determine potential toxicity. Neither dose concentration showed any observable signs of toxicity during or after dosing. Plasma concentrations sampled at pre-dose, 0.5 hour, and 1 hour post dose around the 2nd and 4th doses were analyzed by LC-MS/MS (Table 5). Compound **15** was dosed at 150 and 300 mg/kg QD for 7 days to check for signs of toxicity. Neither dose concentration showed any observable signs of toxicity after 7 days of dosing. Plasma concentrations sampled at pre-dose, 0.5 hour, and 1 hour post dose around the 2nd and 5th doses were analyzed by LC-MS/MS (Table 5). Compound **25** was dosed at 100 and 250 mg/kg QD for 7 days. No signs of toxicity were observed at the 100 mg/kg dose after 7 days. Minor signs of toxicity were observed after the 7th dose of **25** at 250 mg/kg, including slight lethargy and lack of grooming. Plasma levels were collected at 2 hours after the 2nd dose, prior to the 3rd dose, 2 hours after the 5th dose and 24, 48 and 72 hours after the 7th dose and analyzed for compound concentration by LC-MS/MS (Table 5). Blood and organs were collected from all mice after the final dose. Histological analysis of all major organs showed no abnormalities and CBC and serum chemistry results were all within the normal range for mice for both **15** and **25** at both dose concentrations. For compound **6**, CBC and serum chemistry results showed a decrease in the white blood cell counts from 4.8 ± 1.2 K/μL in the untreated controls to 1.5 ± 0.2 K/μL for the 100 mg/kg dosed mice and 1.5 ± 0.9 K/μL for the 200 mg/kg dosed mice. There was also a decrease in lymphocytes in the compound **6** treatments,

from 4,060 ± 1,266 ABS/μL for the untreated controls to 1,194 ± 71 ABS/μL for the 100 mg/kg dosed mice and 1,301 ± 678 ABS/μL for the 200 mg/kg dosed mice. Though there were no visible signs of abnormalities in any of the organs when compared to controls at either dose for compound **6**, some amount of the compound and vehicle was observed to have precipitated and remained in the stomach and small intestines for the 200 mg/kg dose, suggesting that solubility limits may be insurmountable for this compound at higher dose concentrations. However, this is well above the efficacious dose concentration of 8 mg/kg QD, allowing for a reasonably large therapeutic window to continue this compound as a possible treatment candidate.

Compound **25** only left a small therapeutic window between maximum plasma concentrations of 72.2 ± 5.2 μM in the toxicity study and 28.8 ± 8.9 μM at the efficacious 30 mg/kg QD dose. Since minor signs of toxicity were already appearing after 7 doses of **25**, this high systemic exposure would be a limiting factor for its development into a clinical drug for cryptosporidiosis. However, compound **15** had a low maximum plasma concentration of 0.51 ± 0.2 μM at its efficacious dose of 30 mg/kg BID. This is over 30-fold lower than the maximum plasma exposures of 30.5 ± 6.1 μM after the 2nd dose and 34.1 ± 8.6 μM after the 5th dose in the multi-dose toxicity at 300 mg/kg QD. Since there were no signs of toxicity at this high dose of **15**, this compound remains a viable candidate with a wide therapeutic window that is worth further exploration in large animal efficacies and other toxicity screens.

Conclusions

In the present study, we designed a series of AC-scaffold BKIs, which contain variable Ar and R groups. Hydroxyl containing R groups were mainly investigated with the goal of finding compounds that have distinct physiochemical properties compared with the non-hydroxyl containing counterparts. The compounds were screened for potent inhibition of the *Cp*CDPK1

enzyme and in vitro cellular potency. Inhibitors were then screened for the lack of growth inhibition of mammalian cell lines and minimal hERG activity. Inhibitors were further tested for efficacy in a mouse model and compounds that showed no clinical signs of illness were moved to a dose response study. A strong correlation between solubility and in vivo efficacy was found for this class of compounds. Compounds **6** and **15** are both efficacious in the *C. parvum* infected IFN-γ KO mouse model, are not toxic to a variety of human cell lines, are safely administered orally to mice at up to 200 to 300 mg/kg of body weight for 7 days, and did not show cardiotoxicity issues in the in vitro hERG assays. Compounds **6** and **15** are both emerging as potential pre-clinical leads for cryptosporidiosis therapy.

EXPERIMENTAL METHODS

General Synthetic Methods. Unless otherwise stated, all chemicals were purchased from commercial suppliers and used without further purification. Microwave irradiation was performed on a CEM Discover System. Reaction progress was monitored by thin-layer chromatograph on silica gel containing an inert binder and a fluorescent indicator (activated at 254 nm) coated flexible sheet (J. T. Baker). Chromatography was performed using an automated flash chromatography system, eluting on pre-packed silica gel columns with CH_2Cl_2/MeOH or Hexane/Ethyl ester gradient solvent system. The purity of all final compounds was determined by analytical LC-MS using an Onyx Monolithic C18 column (4.6 mm x 100 mm) (Phenomenex, Torrance, CA) and eluting with CH_3CN/H_2O solvent system (+0.1% TFA). The products were detected by UV at 220 nm. All compounds were determined to be >95% pure by this method. The mass spectra were recorded with an Ion Trap Mass Spectrometer (Agilent, Santa Clara, CA). High resolution mass spectrometry (HRMS) was performed on LTQ-Orbitrap (Thermo Fisher) using electrospray source in positive ionization mode and Orbitrap resolution setting of 60,000.

^{1}H NMR spectra were recorded on Bruker 300 or 500 MHz spectrometers at ambient temperature. ^{13}C NMR spectra were recorded on Bruker 126 MHz spectrometer at ambient temperature. Chemical shifts are reported in parts per million (δ) referenced to the internal standards (^{1}H signals: 7.26 ppm for $CDCl_3$, 3.34 ppm for CD_3OD and 2.50 ppm for $(CD_3)_2SO$; ^{13}C signal: 39.51 for $(CD_3)_2SO$) and coupling constants in Hz.

General Synthetic Procedure. Quinoline aldehyde (0.1 mmol, 1 eq), a corresponding hydrazine hydrochloride (0.11 mmol, 1.1 eq) and DIPEA (0.11 mmol, 1.1 eq) were dissolved in EtOH (2 mL) in a microwave tube, purged with N_2, heated to 70°C under microwave for 20 min. After evaporation of the solvent, the product hydrozone was used for the next step directly.

Hydrazone obtained above (0.1 mmol, 1eq) was dissolved in 2 mL DMF and cooled to 0°C, then NBS (0.11 mmol, 1.1 eq) dissolved in 1 mL DMF was added dropwise, the reaction mixture was stirred at 0°C for 20 min.

In another flask, NaH (0.3 mmol, 3 eq) was added to a solution of 2-cyanoacetamide (0.2 mmol, 2 eq) in DMF. After stirring for 20 min, the solution was added to the above bromo-hydrazone solution at 0°C, and the resulted reaction mixture was stirred at r.t. overnight. The solvent was removed; the residue was extracted with CH_2Cl_2, dried over Na_2SO_4, filtered, and concentrated in vacuo. The crude product was then purified via flash chromatography over silica, eluting with a CH_2Cl_2/MeOH gradient. Further purification, if necessary, was performed via preparatory RP-HPLC, eluting with H_2O/CH_3CN gradient (+0.1% TFA).

5-amino-3-(7-ethoxyquinolin-3-yl)-1-(3-hydroxy-2,2-dimethylpropyl)-1H-pyrazole-4-carboxamide (1). Reported previously.[21]

5-amino-3-(2-ethoxyquinolin-6-yl)-1-(3-hydroxy-2,2-dimethylpropyl)-1H-pyrazole-4-carboxamide (2). Reported previously.[21]

5-amino-3-(6-ethoxynaphthalen-2-yl)-1-(3-hydroxy-2,2-dimethylpropyl)-1H-pyrazole-4-carboxamide (3). ^{1}H NMR (500 MHz, $CDCl_3$) δ 7.94 (s, 1H), 7.81 – 7.75 (m, 2H), 7.58 (d, *J* = 8.6 Hz, 1H), 7.19 (d, *J* = 8.6 Hz, 1H), 7.15 (s, 1H), 4.17 (q, *J* = 6.6 Hz, 2H), 3.87 (s, 2H), 3.34 (s, 2H), 1.49 (t, *J* = 6.6 Hz, 3H), 1.05 (s, 6H). ^{13}C NMR (126 MHz, DMSO) δ 166.2, 156.9, 151.6, 147.9, 134.0, 129.6, 128.9, 128.1, 127.5, 127.1, 126.9, 119.3, 106.5, 94.2, 67.4, 63.2, 52.6, 40.0, 37.7, 22.6, 14.6. MS (ESI) $(M+H)^+$=383.6; HRMS (ESI) m/z: calculated for $C_{21}H_{26}N_4O_3$ $[M + H]^+$ 383.2078; observed 383.2083. HPLC analysis: 97.8% purity.

5-amino-3-(7-cyclopropoxyquinolin-3-yl)-1-(3-hydroxy-2,2-dimethylpropyl)-1H-pyrazole-4-carboxamide (4). ^{1}H NMR (500 MHz, MeOD) δ 9.28 (s, 1H), 9.22 (s, 1H), 8.28 (d, *J* = 9.2 Hz, 1H), 7.88 (s, 1H), 7.61 (dd, *J* = 9.2, 1.8 Hz, 1H), 4.20 – 4.13 (m, 1H), 3.95 (s, 1H), 3.32 (s, 1H), 1.06-1.00 (m, 8H), 0.94 – 0.88 (m, 2H). MS (ESI) $(M+H)^+$= 396.5; HRMS (ESI) m/z: calculated for $C_{21}H_{25}N_5O_3$ $[M + H]^+$ 396.2030; observed 396.2026. HPLC analysis: 96.0% purity.

5-amino-3-(2-cyclopropoxyquinolin-6-yl)-1-(3-hydroxy-2,2-dimethylpropyl)-1H-pyrazole-4-carboxamide (5). ^{1}H NMR (500 MHz, $CDCl_3$) δ 8.03 (d, *J* = 8.9 Hz, 1H), 7.99 (d, *J* = 8.5 Hz, 1H), 7.91 (s, 1H), 7.79 (d, *J* = 8.5 Hz, 1H), 6.94 (d, *J* = 8.9 Hz, 1H), 5.27-5.12 (m, 2H), 4.57-4.48 (m, 2H), 3.86 (s, 2H), 3.34 (s, 2H), 1.04 (s, 6H), 0.90 – 0.80 (m, 4H). ^{13}C NMR (126 MHz, DMSO) δ 166.2, 162.6, 151.6, 147.4, 145.8, 139.6, 130.5, 129.7, 127.7, 127.0, 124.8, 113.1, 94.3, 67.4, 52.6, 50.0, 37.7, 22.6, 5.6. MS (ESI) $(M+H)^+$= 396.6; HRMS (ESI) m/z: calculated for $C_{21}H_{25}N_5O_3$ $[M + H]^+$ 396.2030; observed 396.2027. HPLC analysis: 97.0% purity.

5-amino-3-(6-cyclopropoxynaphthalen-2-yl)-1-(3-hydroxy-2,2-dimethylpropyl)-1H-pyrazole-4-carboxamide (6). ^{1}H NMR (500 MHz, DMSO) δ 7.98 (s, 1H), 7.91 (d, J = 8.7 Hz,

2H), 7.58 (d, J = 11.6 Hz, 2H), 7.22 (dd, J = 8.9, 2.0 Hz, 1H), 6.35 (s, 2H), 5.09 (t, J = 5.0 Hz, 1H), 4.03 – 3.94 (m, 1H), 3.80 (s, 2H), 3.21 (d, J = 4.9 Hz, 2H), 0.93 (s, 6H), 0.88 (q, J = 6.1 Hz, 2H), 0.74 (s, 2H). ^{13}C NMR (126 MHz, DMSO) δ 166.7, 157.0, 151.5, 147.8, 133.8, 129.6, 129.0, 128.3, 127.5, 127.1, 126.9, 118.8, 107.9, 94.2, 67.4, 52.6, 50.9, 37.6, 22.5, 5.9. MS (ESI) $(M+H)^+$= 395.6; HRMS (ESI) m/z: calculated for $C_{22}H_{26}N_4O_3$ $[M + H]^+$ 395.2078; observed 395.2074. HPLC analysis: >99.0% purity.

5-amino-3-(7-ethoxyquinolin-3-yl)-1-(4-hydroxybutan-2-yl)-1H-pyrazole-4-carboxamide (7). Reported previously.[21]

5-amino-3-(2-ethoxyquinolin-6-yl)-1-(4-hydroxybutan-2-yl)-1H-pyrazole-4-carboxamide (8). ^{1}H NMR (500 MHz, MeOD) δ 8.18 (d, *J* = 8.8 Hz, 1H), 7.98 (d, *J* = 1.8 Hz, 1H), 7.91 (d, *J* = 8.6 Hz, 1H), 7.78 (dd, *J* = 8.6, 1.9 Hz, 1H), 6.99 (d, *J* = 8.8 Hz, 1H), 4.59 – 4.47 (m, 3H), 3.60 (ddd, *J* = 10.8, 5.9, 4.9 Hz, 1H), 3.42 (ddd, *J* = 10.8, 8.7, 5.2 Hz, 1H), 2.18 (ddt, *J* = 14.4, 9.8, 5.0 Hz, 1H), 2.04 – 1.92 (m, 1H), 1.50 (d, *J* = 6.7 Hz, 3H), 1.46 (t, *J* = 7.1 Hz, 3H). MS (ESI) $(M+H)^+$= 370.8; HRMS (ESI) m/z: calculated for $C_{19}H_{23}N_5O_3$ $[M + H]^+$ 370.1874; observed 370.1871. HPLC analysis: >99.0% purity.

5-amino-3-(6-ethoxynaphthalen-2-yl)-1-(4-hydroxybutan-2-yl)-1H-pyrazole-4-carboxamide (9). ^{1}H NMR (500 MHz, MeOD) δ 7.96 (s, 1H), 7.89 (d, *J* = 8.4 Hz, 1H), 7.84 (d, *J* = 8.9 Hz, 1H), 7.57 (dd, *J* = 8.4, 1.5 Hz, 1H), 7.30 (d, *J* = 2.3 Hz, 1H), 7.21 (dd, *J* = 8.9, 2.3 Hz, 1H), 4.58 – 4.47 (m, 1H), 4.20 (q, *J* = 7.0 Hz, 2H), 3.60 (dt, *J* = 10.8, 5.4 Hz, 1H), 3.42 (ddd, *J* = 10.8, 8.8, 5.2 Hz, 1H), 2.18 (ddt, *J* = 14.4, 9.8, 5.0 Hz, 1H), 2.04 – 1.91 (m, 1H), 1.54 – 1.43 (m, 6H). ^{13}C NMR (126 MHz, DMSO) δ 166.40, 156.9, 150.3, 148.1, 134.0, 129.6, 129.2, 128.1, 127.5, 127.3, 126.8, 119.3, 106.5, 94.5, 63.2, 57.6, 48.2, 38.3, 20.1, 14.6. MS (ESI) $(M+H)^+$= 369.5;

HRMS (ESI) m/z: calculated for $C_{20}H_{24}N_4O_3$ $[M + H]^+$ 369.1921; observed 369.1918. HPLC analysis: >99.0% purity.

5-amino-3-(2-cyclopropoxyquinolin-6-yl)-1-(4-hydroxybutan-2-yl)-1H-pyrazole-4-carboxamide (10). ^{1}H NMR (500 MHz, MeOD) δ 8.24 (d, *J* = 8.9 Hz, 1H), 8.02 (s, 1H), 7.97 (d, *J* = 8.6 Hz, 1H), 7.83 (dd, *J* = 8.6, 1.7 Hz, 1H), 7.06 (d, *J* = 8.9 Hz, 1H), 4.55 (dt, *J* = 9.7, 6.6 Hz, 1H), 4.49 (ddd, *J* = 9.0, 6.2, 3.0 Hz, 1H), 3.61 (dt, *J* = 10.7, 5.4 Hz, 1H), 3.43 (ddd, *J* = 10.8, 8.9, 5.3 Hz, 1H), 2.19 (ddt, *J* = 14.3, 9.7, 4.9 Hz, 1H), 1.99 (tt, *J* = 8.8, 5.7 Hz, 1H), 1.51 (d, *J* = 6.7 Hz, 4H), 0.93 – 0.87 (m, 2H), 0.85-0.79 (m, 2H). MS (ESI) $(M+H)^+$= 382.8; HRMS (ESI) m/z: calculated for $C_{20}H_{23}N_5O_3$ $[M + H]^+$ 382.1874; observed 382.1871. HPLC analysis: 95.0% purity.

5-amino-3-(7-cyclopropoxyquinolin-3-yl)-1-(4-hydroxybutan-2-yl)-1H-pyrazole-4-carboxamide (11). ^{1}H NMR (500 MHz, MeOD) δ 8.97 (d, *J* = 2.1 Hz, 1H), 8.49 (d, *J* = 1.9 Hz, 1H), 7.94 (d, *J* = 9.0 Hz, 2H), 7.76 (d, *J* = 2.3 Hz, 1H), 7.33 (dd, *J* = 9.0, 2.4 Hz, 1H), 4.61 – 4.52 (m, 1H), 4.02 (dq, *J* = 9.0, 2.9 Hz, 1H), 3.65 – 3.58 (m, 1H), 3.43 (ddd, *J* = 10.9, 8.7, 5.2 Hz, 1H), 2.21 (qd, *J* = 9.8, 5.0 Hz, 1H), 2.06 – 1.95 (m, 1H), 1.53 (d, *J* = 6.7 Hz, 3H), 0.98 – 0.92 (m, 2H), 0.86 – 0.79 (m, 2H). MS (ESI) $(M+H)^+$= 382.5; HRMS (ESI) m/z: calculated for $C_{20}H_{23}N_5O_3$ $[M + H]^+$ 382.1874; observed 382.1872. HPLC analysis: 97.0% purity.

5-amino-3-(6-cyclopropoxynaphthalen-2-yl)-1-(4-hydroxybutan-2-yl)-1H-pyrazole-4-carboxamide (12). ^{1}H NMR (500 MHz, MeOD) δ 7.98 (s, 1H), 7.93 (d, *J* = 8.4 Hz, 1H), 7.86 (d, *J* = 8.9 Hz, 1H), 7.60 (d, *J* = 2.1 Hz, 1H), 4.54 (ddd, *J* = 9.6, 6.7, 4.9 Hz, 1H), 3.96 (dq, *J* = 9.0, 2.9 Hz, 1H), 3.61 (dt, *J* = 10.8, 5.4 Hz, 1H), 3.43 (ddd, *J* = 10.9, 8.7, 5.2 Hz, 1H), 2.19 (ddt, *J* = 14.4, 9.8, 5.0 Hz, 1H), 2.07 – 1.94 (m, 1H), 1.12 – 0.50 (m, 2H). ^{13}C NMR (126 MHz, DMSO) δ 166.0, 157.0, 149.9, 147.7, 133.6, 129.8, 129.7, 128.9, 127.5, 127.3, 126.8, 118.9, 107.9, 94.5,

57.40, 50.87, 48.00, 38.20, 20.14, 5.98. MS (ESI) $(M+H)^+$= 381.5; HRMS (ESI) m/z: calculated for $C_{21}H_{24}N_4O_3$ $[M + H]^+$ 381.1921; observed 381.1923. HPLC analysis: 98.0% purity.

5-amino-3-(7-ethoxyquinolin-3-yl)-1-(4-hydroxy-2-methylbutan-2-yl)-1H-pyrazole-4-carboxamide (13). ^{1}H NMR (500 MHz, MeOD) δ 9.25 (d, *J* = 1.5 Hz, 1H), 9.21 (s, 1H), 8.27 (d, *J* = 9.2 Hz, 1H), 7.59 (dd, *J* = 9.2, 2.0 Hz, 1H), 7.49 (d, *J* = 1.5 Hz, 1H), 4.39 – 4.32 (m, 2H), 3.56 (t, *J* = 7.1 Hz, 2H), 2.27 (t, *J* = 7.1 Hz, 2H), 1.72 (s, 6H), 1.54 (t, *J* = 7.0 Hz, 3H). MS (ESI) $(M+H)^+$= 384.8; HRMS (ESI) m/z: calculated for $C_{20}H_{25}N_5O_3$ $[M + H]^+$ 384.2030; observed 384.2026. HPLC analysis: 96.2 % purity.

5-amino-3-(2-ethoxyquinolin-6-yl)-1-(4-hydroxy-2-methylbutan-2-yl)-1H-pyrazole-4-carboxamide (14). ^{1}H NMR (500 MHz, MeOD) δ 8.19 (d, *J* = 8.7 Hz, 1H), 7.98 (s, 1H), 7.90 (d, *J* = 8.5 Hz, 1H), 7.79 (d, *J* = 8.4 Hz, 1H), 7.00 (d, *J* = 8.8 Hz, 1H), 4.55 (q, *J* = 6.8 Hz, 2H), 3.60 (t, *J* = 6.8 Hz, 2H), 2.28 (t, *J* = 6.8 Hz, 2H), 1.73 (s, 6H), 1.47 (t, *J* = 6.8 Hz, 3H). MS (ESI) $(M+H)^+$= 384.6; HRMS (ESI) m/z: calculated for $C_{20}H_{25}N_5O_3$ $[M + H]^+$ 384.2030; observed 384.2031. HPLC analysis: 96.5% purity.

5-amino-3-(6-ethoxynaphthalen-2-yl)-1-(4-hydroxy-2-methylbutan-2-yl)-1H-pyrazole-4-carboxamide (15). ^{1}H NMR (500 MHz, MeOD) δ 7.95 (s, 1H), 7.88 (d, *J* = 8.3 Hz, 1H), 7.84 (d, *J* = 8.9 Hz, 1H), 7.56 (d, *J* = 8.3 Hz, 1H), 7.30 (s, 1H), 7.20 (d, *J* = 8.9 Hz, 1H), 4.20 (q, *J* = 6.7 Hz, 2H), 3.60 (t, *J* = 6.9 Hz, 2H), 2.27 (t, *J* = 6.9 Hz, 2H), 1.72 (s, 6H), 1.49 (t, *J* = 6.7 Hz, 3H). ^{13}C NMR (126 MHz, DMSO) δ 166.7, 156.8, 150.4, 145.8, 133.9, 129.5, 129.1, 128.0, 127.5, 127.2, 126.8, 119.2, 106.5, 95.7, 63.1, 60.1, 57.0, 42.5, 27.2, 14.5. MS (ESI) $(M+H)^+$= 383.5; HRMS (ESI) m/z: calculated for $C_{21}H_{26}N_4O_3$ $[M + H]^+$ 383.2078; observed 383.2075. HPLC analysis: 98.9% purity.

5-amino-3-(7-cyclopropoxyquinolin-3-yl)-1-(4-hydroxy-2-methylbutan-2-yl)-1H-pyrazole-4-carboxamide (16). ^{1}H NMR (500 MHz, $CDCl_3$) δ 9.03 (s, 1H), 8.29 (s, 1H), 7.82 (s, 1H), 7.77 (d, *J* = 8.9 Hz, 1H), 7.26 (d, *J* = 8.9 Hz, 1H), 5.85 (s, 2H), 5.24 (s, 2H), 3.97-3.92 (m, 1H), 3.77 (t, *J* = 6.0 Hz, 2H), 2.29 (t, *J* = 6.0 Hz, 2H), 1.76 (s, 6H), 0.96-0.91 (m, 2H), 0.91-0.87 (m, 2H). MS (ESI) $(M+H)^+$= 396.5; HRMS (ESI) m/z: calculated for $C_{21}H_{25}N_5O_3$ $[M + H]^+$ 396.2030; observed 396.2030. HPLC analysis: 96.9% purity.

5-amino-3-(2-cyclopropoxyquinolin-6-yl)-1-(4-hydroxy-2-methylbutan-2-yl)-1H-pyrazole-4-carboxamide (17). ^{1}H NMR (500 MHz, MeOD) δ 8.22 (d, *J* = 8.9 Hz, 1H), 8.00 (d, *J* = 1.7 Hz, 1H), 7.95 (d, *J* = 8.6 Hz, 1H), 7.82 (dd, *J* = 8.6, 1.7 Hz, 1H), 7.04 (d, *J* = 8.9 Hz, 1H), 4.48 (tt, *J* = 6.3, 3.0 Hz, 1H), 3.60 (t, *J* = 7.2 Hz, 2H), 2.28 (t, *J* = 7.2 Hz, 2H), 1.73 (s, 6H), 0.93 – 0.86 (m, 2H), 0.84 – 0.76 (m, 2H). MS (ESI) $(M+H)^+$= 396.7; HRMS (ESI) m/z: calculated for $C_{21}H_{25}N_5O_3$ $[M + H]^+$ 396.2030; observed 396.2027. HPLC analysis: 97.5% purity.

5-amino-3-(6-cyclopropoxynaphthalen-2-yl)-1-(4-hydroxy-2-methylbutan-2-yl)-1H-pyrazole-4-carboxamide (18). ^{1}H NMR (500 MHz, MeOD) δ 7.97 (s, 1H), 7.92 (d, *J* = 8.4 Hz, 1H), 7.85 (d, *J* = 8.9 Hz, 1H), 7.61 – 7.55 (m, 2H), 7.22 (dd, *J* = 8.9, 2.2 Hz, 1H), 4.00 – 3.91 (m, 1H), 3.61 (t, *J* = 7.2 Hz, 2H), 2.28 (t, *J* = 7.2 Hz, 2H), 1.73 (s, 6H), 0.93-0.87 (M, 2H), 0.82 – 0.75 (m, 2H). MS (ESI) $(M+H)^+$= 395.8; HRMS (ESI) m/z: calculated for $C_{22}H_{26}N_4O_3$ $[M + H]^+$ 395.2078; observed 395.2075. HPLC analysis: 96.0% purity.

5-amino-3-(7-ethoxyquinolin-3-yl)-1-(1-hydroxy-2-methylpropan-2-yl)-1H-pyrazole-4-carboxamide (19). ^{1}H NMR (500 MHz, MeOD) δ 9.28 (d, *J* = 1.3 Hz, 1H), 9.23 (s, 1H), 8.28 (d, *J* = 9.2 Hz, 1H), 7.61 (dd, *J* = 9.2, 2.2 Hz, 1H), 7.50 (s, 1H), 4.37 (q, *J* = 7.0 Hz, 3H), 3.89 (s, 2H), 1.66 (s, 6H), 1.56 (t, *J* = 7.0 Hz, 4H). MS (ESI) $(M+H)^+$= 370.5; HRMS (ESI) m/z:

calculated for $C_{19}H_{23}N_5O_3$ $[M + H]^+$ 370.1874; observed 370.1870. HPLC analysis: 95.0% purity.

5-amino-3-(2-ethoxyquinolin-6-yl)-1-(1-hydroxy-2-methylpropan-2-yl)-1H-pyrazole-4-carboxamide (20). ^{1}H NMR (500 MHz, MeOD) δ 8.19 (d, *J* = 8.8 Hz, 1H), 7.99 (s, 1H), 7.91 (d, *J* = 8.6 Hz, 1H), 7.80 (d, *J* = 8.6 Hz, 1H), 7.00 (d, *J* = 8.8 Hz, 1H), 4.55 (q, *J* = 7.0 Hz, 2H), 3.89 (s, 2H), 1.65 (s, 6H), 1.47 (t, *J* = 7.0 Hz, 3H). ^{13}C NMR (126 MHz, DMSO) δ 166.5, 161.8, 151.0, 145.7, 139.3, 130.4, 129.6, 127.6, 126.7, 124.5, 113.4, 95.8, 68.4, 62.4, 61.2, 23.5, 14.3. MS (ESI) $(M+H)^+$= 370.8; HRMS (ESI) m/z: calculated for $C_{19}H_{23}N_5O_3$ $[M + H]^+$ 370.1874; observed 370.1871. HPLC analysis: 98.3% purity.

5-amino-3-(6-ethoxynaphthalen-2-yl)-1-(1-hydroxy-2-methylpropan-2-yl)-1H-pyrazole-4-carboxamide (21). ^{1}H NMR (500 MHz, MeOD) δ 8.12 (s, 1H), 7.98 (d, *J* = 8.4 Hz, 1H), 7.91 (d, *J* = 8.9 Hz, 1H), 7.61 (d, *J* = 8.4 Hz, 1H), 7.35 (s, 1H), 7.26 (dd, *J* = 8.9, 1.4 Hz, 1H), 4.21 (q, *J* = 7.0 Hz, 2H), 3.93 (d, *J* = 1.1 Hz, 2H), 1.71 (d, *J* = 1.8 Hz, 6H), 1.48 (t, *J* = 7.0 Hz, 3H). ^{13}C NMR (126 MHz, DMSO) δ 166.6, 156.9, 151.1, 146.6, 146.2, 134.0, 129.6, 129.1, 128.1, 127.6, 127.3, 126.8, 119.3, 106.5, 95.7, 68.4, 63.2, 62.4, 23.6, 14.6. MS (ESI) $(M+H)^+$= 369.7; HRMS (ESI) m/z: calculated for $C_{20}H_{24}N_4O_3$ $[M + H]^+$ 369.1921; observed 369.1919. HPLC analysis: >99.0% purity.

5-amino-3-(7-cyclopropoxyquinolin-3-yl)-1-(1-hydroxy-2-methylpropan-2-yl)-1H-pyrazole-4-carboxamide (22). ^{1}H NMR (500 MHz, MeOD) δ 9.31 (s, 1H), 9.23 (s, 1H), 8.32 – 8.25 (m, 1H), 7.86 (d, *J* = 13.1 Hz, 1H), 7.62 (d, *J* = 9.0 Hz, 1H), 4.20-4.13 (m, 1H), 3.90 (s, 2H), 1.67 (s, 6H), 1.06-1.01 (m, 2H), 0.95-0.89 (m, 2H). MS (ESI) $(M+H)^+$= 382.5; HRMS (ESI) m/z: calculated for $C_{20}H_{23}N_5O_3$ $[M + H]^+$ 382.1874; observed 382.1871. HPLC analysis: 98.4% purity.

5-amino-3-(2-cyclopropoxyquinolin-6-yl)-1-(1-hydroxy-2-methylpropan-2-yl)-1H-pyrazole-4-carboxamide (23). ^{1}H NMR (500 MHz, MeOD) δ 8.92 (d, *J* = 9.2 Hz, 1H), 8.35 (d, *J* = 1.6 Hz, 1H), 8.18 (dd, *J* = 8.7, 1.8 Hz, 1H), 8.00 (d, *J* = 8.7 Hz, 1H), 7.82 (d, *J* = 9.2 Hz, 1H), 4.61 (dq, *J* = 8.9, 3.1 Hz, 1H), 3.89 (s, 2H), 1.65 (s, 6H), 1.12 – 1.05 (m, 4H). ^{13}C NMR (126 MHz, DMSO) δ 166.6, 162.6, 151.1, 145.9, 145.8, 139.6, 130.6, 129.9, 127.7, 126.9, 124.8, 113.1, 95.8, 68.4, 62.5, 50.0, 23.6, 5.6. MS (ESI) $(M+H)^+$= 382.7; HRMS (ESI) m/z: calculated for $C_{20}H_{23}N_5O_3$ $[M + H]^+$ 382.1874; observed 382.1870. HPLC analysis: >99.0% purity.

5-amino-3-(6-cyclopropoxynaphthalen-2-yl)-1-(1-hydroxy-2-methylpropan-2-yl)-1H-pyrazole-4-carboxamide (24). ^{1}H NMR (500 MHz, MeOD) δ 8.12 (s, 1H), 8.01 (d, *J* = 8.5 Hz, 1H), 7.92 (d, *J* = 9.0 Hz, 1H), 7.65 – 7.60 (m, 2H), 7.27 (dd, *J* = 8.9, 2.3 Hz, 1H), 3.97 (ddd, *J* = 9.0, 5.9, 2.8 Hz, 1H), 3.93 (s, 2H), 1.71 (s, 6H), 0.91 (dt, *J* = 11.7, 5.9 Hz, 2H), 0.80 – 0.76 (m, 2H). ^{13}C NMR (126 MHz, DMSO) δ 166.6, 157.0, 151.1, 146.5, 133.8, 129.7, 129.3, 128.4, 127.7, 127.3, 126.9, 118.9, 107.9, 95.7, 68.4, 62.5, 51.0, 23.6, 6.0. MS (ESI) $(M+H)^+$= 381.7; HRMS (ESI) m/z: calculated for $C_{21}H_{24}N_4O_3$ $[M + H]^+$ 381.1921; observed 381.1918. HPLC analysis: 98.0% purity.

5-amino-1-(tert-butyl)-3-(6-cyclopropoxynaphthalen-2-yl)-1H-pyrazole-4-carboxamide (25). Reported previously.[21]

5-amino-1-(tert-butyl)-3-(6-(prop-2-yn-1-yloxy)naphthalen-2-yl)-1H-pyrazole-4-carboxamide (26). ^{1}H NMR (500 MHz, $CDCl_3$) δ 8.00 (s, 1H), 7.84 (dd, *J* = 13.9, 8.7 Hz, 2H), 7.65 (dd, *J* = 8.4, 1.1 Hz, 1H), 7.29 (s, 1H), 7.25 (dd, *J* = 8.9, 2.4 Hz, 1H), 5.72 (s, 2H), 5.32 (s, 2H), 4.85 (d, *J* = 2.3 Hz, 2H), 2.60 (t, *J* = 2.3 Hz, 1H), 1.72 (s, 9H). MS (ESI) $(M+H)^+$= 363.8; HRMS (ESI) m/z: calculated for $C_{21}H_{22}N_4O_2$ $[M + H]^+$ 363.1816; observed 363.1813. HPLC analysis: 97.6% purity.

5-amino-1-(cyclopropylmethyl)-3-(6-ethoxynaphthalen-2-yl)-1H-pyrazole-4-carboxamide (27). Reported previously.[16]

Pharmacokinetic analysis in adult mice. Mouse oral PK studies were performed as previously described using three female BALB/c mice (10-12 weeks old) in each group.[24] Each group received an individual BKI at a dose of 10 or 25 mg/kg of body weight dissolved in 3% ethanol/7% Tween 80/90% saline by oral gavage. Blood samples were taken by tail bleeding into heparinized tubes at designated time points and centrifuged to obtain plasma. The samples were frozen at -20°C. The test compounds were extracted from the plasma samples using acetonitrile/0.1% formic acid with an internal standard. A standard mix of all test compounds was prepared for comparison and quantification. The compounds were quantified by LC-MS/MS analysis. PK calculations of C_{max}, time at which C_{max} is observed (T_{max}), AUC, oral clearance, and half-life were performed using Pharsight Phoenix WinNonlin software (Certara, St. Louis, MO, USA).

Fecal concentration analysis in adult mice. Fecal concentrations were determined as previously described.[20] Three female BALB/c mice (10-12 weeks old) were used in each group. Each group received an individual BKI at a dose of 25 mg/kg of body weight dissolved in 3% ethanol/7% Tween 80/90% saline by oral gavage. Feces were collected for 24 h, weighed and soaked overnight in 3 mL of DPBS per gram of feces. Feces were homogenized and an internal standard added. The test compounds and internal standard were extracted from the fecal samples using acetonitrile. The samples were centrifuged for 30 min at 2000 *g*. Supernatant was removed and concentrated by repeated evaporation in a Savant SPD121P SpeedVac Concentrator (Thermo Scientific, Waltham, MA, USA) and reconstitution in acetonitrile. A standard mix of all test compounds was prepared for comparison and quantification. The compounds were quantified by LC-MS/MS analysis and the fecal concentration was calculated.

Plasma protein binding. Plasma protein binding was determined as previously described.[24] Dialysis membrane sheets (MW cutoff 3.5 kDa) (HTDialysis, LLC, Gales Ferry, CT, USA) were soaked for 1 h in DPBS and then in 20% ethanol for 30 min. The membrane was clamped between two Teflon plates containing a row of opposing wells. Test compound in DMSO was added to 0.12 mL of serum to a concentration of 5 μM; a small aliquot was taken as a 100% recovery standard and the solution was placed on one side of the membrane. The well on the other side of the membrane was charged with an equal volume of DPBS, and the block was placed on an orbital shaker for 18 h at 37°C. An aliquot was taken from each side of the membrane. All aliquots were matrix adjusted, internal standard in acetonitrile was added to each aliquot, and the samples were centrifuged to precipitate protein. Test compound in the supernatants was quantified by LC-MS/MS analysis to determine the concentration on each side of the membrane and the total recovery of test compound from the device. A control dialysis was carried out with dialysis buffer on both sides of the membrane and test compound on one side to ensure that equilibration across the membrane was achieved. The fraction of compound bound to protein was calculated as bound/(unbound + bound).

***Cp*CDPK1 enzyme inhibition of BKIs.** *C.p* CDPK1 enzyme inhibition and IC_{50} determination of BKIs was determined by measuring ATP consumption in a coupled reaction for phosphate group incorporation to biotinylated Syntide-2 (BioSyntide-2) peptide substrate (Biotin-C6-PLARTLSVAGLPGKK) (American Peptide Company, Inc. Sunnyvale, CA) in the presence or absence of inhibitors as previously described.[10] All assays were performed in a buffered solution containing 1 mM EGTA (pH 7.2), 10 mM $MgCl_2$, 20 mM HEPES pH 7.5 (KOH), 0.1% BSA and enzyme activation reagent containing 2 mM $CaCl_2$. The final reaction volume of 25 μL contained 20 μM BioSyntide-2, 2.1 μM *Cp*CDPK1, with or without serial dilutions of inhibitors. The

reaction was initiated with the addition of ATP at 10 μM final concentration. Internal positive and negative controls were included in each assay plate. Reaction mixture was incubated at 30°C and 90 rpm for 90 min. Subsequent changes to initial ATP concentration were measured by a non-radioactive Kinaseglo® luciferase reagent (Promega, Madison, WI) as a luminescence readout using an EnVision Multilabel Plate Reader (Perkin Elmer, Waltham, MA).

BKI inhibition of Nanoluciferase-expressing *C. parvum* growth. Inhibition of *C. parvum* growth and EC_{50} determinations were performed with a Nluc-expressing *C. parvum* parasite in HCT-8 cells as previously described.[20, 25] Briefly, oocysts were propagated in IFN-γ KO mice and isolated from stools by sucrose suspension and cesium chloride gradient. HCT-8 cells were seeded to a 96 or 384-well plate and allowed to grow for 72 h to reach 90-100% confluence. Oocysts were activated by 10-15 min incubation in 10% bleach (0.6% sodium hypochlorite) at room temperature and then washed with DPBS. 500-2000 oocysts per well, depending on the plate type and volume per well used, were applied to plates with RPMI-1640 medium supplemented with 10% heat inactivated horse serum and 1% penicillin/streptomycin at the same time as compound addition. The compound and the oocysts were left in place for the full 72 h growth time. The amount of luciferase-induced light emission was determined by lysing the cell monolayer, adding Nano-Glo® luciferase reagent (Promega, Madison, WI, USA), and reading on an EnVision Multilabel Plate Reader (Perkin Elmer, Waltham, MA, USA). Controls included infected wells with no addition of BKI or any other inhibitor and the background was taken as wells where no *C. parvum* was added. The percentage of growth versus infected cells with no inhibitor was calculated for each concentration of BKI and the half maximal effective concentration (EC_{50}) values were determined by a sigmoidal dose response with variable slope using GraphPad Prism version 6.07

(GraphPad Software, La Jolla, California, USA). Assays were performed 2-3 times, and were expressed as the mean of the values determined.

Efficacy in adult interferon-γ knock-out mice. IFN-γ KO mice (B6.129S7-Ifngtm1Ts/J, Jackson Laboratories), aged 8-10 weeks, were infected by oral gavage (PO) with 1,000 to 10,000 UGA1 Nluc-expressing *C. parvum* oocysts in 0.1 mL DPBS as previously described.[20] Beginning on day 6 post infection (p.i.), mice were dosed PO with BKI suspended in 0.2 mL oral vehicle (3% ethanol/7% Tween 80/90% saline) or vehicle only once daily for 5 days. Mice were moved to clean cages after each dose and fecal collection. Feces were collected daily and weighed from each group during dosing and twice weekly out to 20 to 21 days p.i. Each fecal sample was checked for luminescence on day of collection and RLU readings were normalized to fecal sample weights. Controls groups were dosed with vehicle only and 60 or 100 mg/kg of BKI 1369 to establish an appropriate dynamic range between untreated and successfully treated infections for different experiments.[14] Mice were euthanized if they showed weight loss of ≥20% or other prominent signs of toxicity, strong discomfort, or distress according to the University of Washington's Institutional Animal Care and Use Committee guidelines.

Animal ethics statement. All animal experiments conducted at the University of Washington, USA were approved by the Institutional Animal Care and Use Committee. All animals used in these studies were handled in strict accordance with practices made to minimize suffering.

ASSOCIATED CONTENT

Supporting Information Available: This material is available free of charge via the internet at http://pubs.acs.org.

Synthesis and characterization data for all intermediate compounds;

NMR spectra for final compounds;

Molecular formula strings of studied compounds including assay data.

Corresponding authors:

For Wesley C. Van Voorhis: E-mail: wesley@uw.edu; For Erkang Fan: E-mail: erkang@uw.edu

ACKNOWLEDGEMENTS

The authors thank Geno De Hostos and Robert Choy from PATH Drug Solutions (San Francisco, CA, USA) for their consultation in the drug development pathway and James J. Lynch, Dale J. Kempf, and Gail M. Freiberg (AbbVie) for establishing hERG inhibition of the BKIs. Research studies reported in this publication were supported by National Institute of Allergy and Infectious Diseases (NIAID) of the National Institutes of Health (NIH), USA, under award numbers R01AI089441, R01AI111341 and R01HD080670. The work was also supported by award number 2014-06183 from the United States Department of Agriculture National Institute of Food and Agriculture.

CONFLICT OF INTEREST

Dr. Wesley Van Voorhis is an officer and owns stock in ParaTheraTech Inc., a company that is trying to bring BKIs to the animal health market. He helped design the experiments and edited the paper, but did not have a role in performing or interpreting the results.

Abbreviations List: AUC, area under plasma concentration time curve; ATP, adenosine triphosphate; CDPK1, calcium-dependent protein kinase 1; C_{max}, maximum plasma concentration; *Cp*CDPK1, *Cryptosporidium parvum* CDPK1; DMF, dimethylformamide; EC_{50}, half maximal effective concentration; hERG, human Ether-à-go-go-Related Gene; IC_{50}, half maximal inhibitory concentration; PK, pharmacokinetic; T_{max}, time at which maximum concentration is reached.

REFERENCES

1. Checkley, W.; White, A. C.; Jaganath, D.; Arrowood, M. J.; Chalmers, R. M.; Chen, X.-M.; Fayer, R.; Griffiths, J. K.; Guerrant, R. L.; Hedstrom, L.; Huston, C. D.; Kotloff, K. L.; Kang, G.; Mead, J. R.; Miller, M.; Petri, W. A.; Priest, J. W.; Roos, D. S.; Striepen, B.; Thompson, R. C. A.; Ward, H. D.; Van Voorhis, W. A.; Xiao, L.; Zhu, G.; Houpt, E. R., A review of the global burden, novel diagnostics, therapeutics, and vaccine targets for cryptosporidium. *The Lancet Infectious Diseases* **2015,** *15* (1), 85-94.
2. Kotloff, K. L.; Nataro, J. P.; Blackwelder, W. C.; Nasrin, D.; Farag, T. H.; Panchalingam, S.; Wu, Y.; Sow, S. O.; Sur, D.; Breiman, R. F.; Faruque, A. S. G.; Zaidi, A. K. M.; Saha, D.; Alonso, P. L.; Tamboura, B.; Sanogo, D.; Onwuchekwa, U.; Manna, B.; Ramamurthy, T.; Kanungo, S.; Ochieng, J. B.; Omore, R.; Oundo, J. O.; Hossain, A.; Das, S. K.; Ahmed, S.; Qureshi, S.; Quadri, F.; Adegbola, R. A.; Antonio, M.; Hossain, M. J.; Akinsola, A.; Mandomando, I.; Nhampossa, T.; Acácio, S.; Biswas, K.; O'Reilly, C. E.; Mintz, E. D.; Berkeley, L. Y.; Muhsen, K.; Sommerfelt, H.; Robins-Browne, R. M.; Levine, M. M., Burden and aetiology of diarrhoeal disease in infants and young children in developing countries (the Global Enteric Multicenter Study, GEMS): a prospective, case-control study. *The Lancet* **2013,** *382* (9888), 209-222.
3. Platts-Mills, J. A.; Babji, S.; Bodhidatta, L.; Gratz, J.; Haque, R.; Havt, A.; McCormick, B. J. J.; McGrath, M.; Olortegui, M. P.; Samie, A.; Shakoor, S.; Mondal, D.; Lima, I. F. N.; Hariraju, D.; Rayamajhi, B. B.; Qureshi, S.; Kabir, F.; Yori, P. P.; Mufamadi, B.; Amour, C.; Carreon, J. D.; Richard, S. A.; Lang, D.; Bessong, P.; Mduma, E.; Ahmed, T.; Lima, A. A. A. M.; Mason, C. J.; Zaidi, A. K. M.; Bhutta, Z. A.; Kosek, M.; Guerrant, R. L.; Gottlieb, M.; Miller, M.; Kang, G.; Houpt, E. R., Pathogen-specific burdens of community diarrhoea in developing countries: a multisite birth cohort study (MAL-ED). *The Lancet Global Health* **2015,** *3* (9), e564-e575.
4. Rossignol, J.-F. A.; Ayoub, A.; Ayers, M. S., Treatment of diarrhea caused by Cryptosporidium parvum: A prospective randomized, double-blind, placebo-controlled study of Nitazoxanide. *The Journal of Infectious Diseases* **2001,** *184* (1), 103-106.
5. Amadi, B.; Mwiya, M.; Musuku, J.; Watuka, A.; Sianongo, S.; Ayoub, A.; Kelly, P., Effect of nitazoxanide on morbidity and mortality in Zambian children with cryptosporidiosis: a randomised controlled trial. *The Lancet* **2002,** *360* (9343), 1375-1380.
6. Sparks, H.; Nair, G.; Castellanos-Gonzalez, A.; White, A. C., Treatment of Cryptosporidium: What we know, gaps, and the way forward. *Current Tropical Medicine Reports* **2015,** *2* (3), 181-187.
7. Lourido, S.; Tang, K.; Sibley, L. D., Distinct signalling pathways control Toxoplasma egress and host‐cell invasion. *The EMBO Journal* **2012,** *31* (24), 4524-4534.
8. Ojo, K. K.; Larson, E. T.; Keyloun, K. R.; Castaneda, L. J.; DeRocher, A. E.; Inampudi, K. K.; Kim, J. E.; Arakaki, T. L.; Murphy, R. C.; Zhang, L.; Napuli, A. J.; Maly, D. J.; Verlinde, C. L. M. J.; Buckner, F. S.; Parsons, M.; Hol, W. G. J.; Merritt, E. A.; Van Voorhis, W. C., Toxoplasma gondii calcium-dependent protein kinase 1 is a target for selective kinase inhibitors. *Nature Structural &Amp; Molecular Biology* **2010,** *17*, 602.

9. Kieschnick, H.; Wakefield, T.; Narducci, C. A.; Beckers, C., Toxoplasma gondii attachment to host cells Is regulated by a calmodulin-like domain protein kinase. *Journal of Biological Chemistry* **2001,** *276* (15), 12369-12377.
10. Murphy, R. C.; Ojo, K. K.; Larson, E. T.; Castellanos-Gonzalez, A.; Perera, B. G. K.; Keyloun, K. R.; Kim, J. E.; Bhandari, J. G.; Muller, N. R.; Verlinde, C. L. M. J.; White, A. C.; Merritt, E. A.; Van Voorhis, W. C.; Maly, D. J., Discovery of potent and selective inhibitors of CDPK1 from C. parvum and T. gondii. *ACS Medicinal Chemistry Letters* **2010,** *1* (7), 331-335.
11. Castellanos-Gonzalez, A.; White, J. A. C.; Ojo, K. K.; Vidadala, R. S. R.; Zhang, Z.; Reid, M. C.; Fox, A. M. W.; Keyloun, K. R.; Rivas, K.; Irani, A.; Dann, S. M.; Fan, E.; Maly, D. J.; Van Voorhis, W. C., A novel calcium-dependent protein kinase inhibitor as a lead compound for treating Cryptosporidiosis. *The Journal of Infectious Diseases* **2013,** *208* (8), 1342-1348.
12. Castellanos-Gonzalez, A.; Sparks, H.; Nava, S.; Huang, W.; Zhang, Z.; Rivas, K.; Hulverson, M. A.; Barrett, L. K.; Ojo, K. K.; Fan, E.; Van Voorhis, W. C.; White, J. A. C., A novel calcium-dependent kinase inhibitor, bumped kinase inhibitor 1517, cures Cryptosporidiosis in immunosuppressed mice. *The Journal of Infectious Diseases* **2016,** *214* (12), 1850-1855.
13. Schaefer, D. A.; Betzer, D. P.; Smith, K. D.; Millman, Z. G.; Michalski, H. C.; Menchaca, S. E.; Zambriski, J. A.; Ojo, K. K.; Hulverson, M. A.; Arnold, S. L. M.; Rivas, K. L.; Vidadala, R. S. R.; Huang, W.; Barrett, L. K.; Maly, D. J.; Fan, E.; Van Voorhis, W. C.; Riggs, M. W., Novel bumped kinase inhibitors are safe and effective therapeutics in the calf clinical model for Cryptosporidiosis. *The Journal of Infectious Diseases* **2016,** *214* (12), 1856-1864.
14. Hulverson, M. A.; Choi, R.; Arnold, S. L. M.; Schaefer, D. A.; Hemphill, A.; McCloskey, M. C.; Betzer, D. P.; Müller, J.; Vidadala, R. S. R.; Whitman, G. R.; Rivas, K. L.; Barrett, L. K.; Hackman, R. C.; Love, M. S.; McNamara, C. W.; Shaughnessy, T. K.; Kondratiuk, A.; Kurnick, M.; Banfor, P. N.; Lynch, J. J.; Freiberg, G. M.; Kempf, D. J.; Maly, D. J.; Riggs, M. W.; Ojo, K. K.; Van Voorhis, W. C., Advances in bumped kinase inhibitors for human and animal therapy for cryptosporidiosis. *International Journal for Parasitology* **2017,** *47* (12), 753-763.
15. Vidadala, R. S. R.; Golkowski, M.; Hulverson, M. A.; Choi, R.; McCloskey, M. C.; Whitman, G. R.; Huang, W.; Arnold, S. L. M.; Barrett, L. K.; Fan, E.; Merritt, E. A.; Van Voorhis, W. C.; Ojo, K. K.; Maly, D. J., 7H-pyrrolo[2,3-d]pyrimidin-4-amine-based inhibitors of calcium-dependent protein kinase 1 have distinct inhibitory and oral pharmacokinetic characteristics compared with 1H-pyrazolo[3,4-d]pyrimidin-4-amine-based inhibitors. *ACS Infectious Diseases* **2018,** *4* (4), 516-522.
16. Huang, W.; Choi, R.; Hulverson, M. A.; Zhang, Z.; McCloskey, M. C.; Schaefer, D. A.; Whitman, G. R.; Barrett, L. K.; Vidadala, R. S. R.; Riggs, M. W.; Maly, D. J.; Van Voorhis, W. C.; Ojo, K. K.; Fan, E., 5-Aminopyrazole-4-carboxamide-based compounds prevent the growth of Cryptosporidium parvum. *Antimicrobial Agents and Chemotherapy* **2017,** *61* (8), e00020-17.

17. Zhang, Z.; Ojo, K. K.; Vidadala, R.; Huang, W.; Geiger, J. A.; Scheele, S.; Choi, R.; Reid, M. C.; Keyloun, K. R.; Rivas, K.; Kallur Siddaramaiah, L.; Comess, K. M.; Robinson, K. P.; Merta, P. J.; Kifle, L.; Hol, W. G. J.; Parsons, M.; Merritt, E. A.; Maly, D. J.; Verlinde, C. L. M. J.; Van Voorhis, W. C.; Fan, E., Potent and selective inhibitors of CDPK1 from T. gondii and C. parvum based on a 5-aminopyrazole-4-carboxamide scaffold. *ACS Medicinal Chemistry Letters* **2014,** *5* (1), 40-44.
18. Ojo, K. K.; Eastman, R. T.; Vidadala, R.; Zhang, Z.; Rivas, K. L.; Choi, R.; Lutz, J. D.; Reid, M. C.; Fox, A. M. W.; Hulverson, M. A.; Kennedy, M.; Isoherranen, N.; Kim, L. M.; Comess, K. M.; Kempf, D. J.; Verlinde, C. L. M. J.; Su, X.-z.; Kappe, S. H. I.; Maly, D. J.; Fan, E.; Van Voorhis, W. C., A specific inhibitor of PfCDPK4 blocks malaria transmission: chemical-genetic validation. *The Journal of Infectious Diseases* **2014,** *209* (2), 275-284.
19. Huang, W.; Hulverson, M. A.; Zhang, Z.; Choi, R.; Hart, K. J.; Kennedy, M.; Vidadala, R. S. R.; Maly, D. J.; Van Voorhis, W. C.; Lindner, S. E.; Fan, E.; Ojo, K. K., 5-Aminopyrazole-4-carboxamide analogues are selective inhibitors of Plasmodium falciparum microgametocyte exflagellation and potential malaria transmission blocking agents. *Bioorganic & Medicinal Chemistry Letters* **2016,** *26* (22), 5487-5491.
20. Hulverson, M. A.; Vinayak, S.; Choi, R.; Schaefer, D. A.; Castellanos-Gonzalez, A.; Vidadala, R. S. R.; Brooks, C. F.; Herbert, G. T.; Betzer, D. P.; Whitman, G. R.; Sparks, H. N.; Arnold, S. L. M.; Rivas, K. L.; Barrett, L. K.; White, J. A. C.; Maly, D. J.; Riggs, M. W.; Striepen, B.; Van Voorhis, W. C.; Ojo, K. K., Bumped-kinase inhibitors for Cryptosporidiosis therapy. *The Journal of Infectious Diseases* **2017,** *215* (8), 1275-1284.
21. Huang, W.; Ojo, K. K.; Zhang, Z.; Rivas, K.; Vidadala, R. S. R.; Scheele, S.; DeRocher, A. E.; Choi, R.; Hulverson, M. A.; Barrett, L. K.; Bruzual, I.; Siddaramaiah, L. K.; Kerchner, K. M.; Kurnick, M. D.; Freiberg, G. M.; Kempf, D.; Hol, W. G. J.; Merritt, E. A.; Neckermann, G.; de Hostos, E. L.; Isoherranen, N.; Maly, D. J.; Parsons, M.; Doggett, J. S.; Van Voorhis, W. C.; Fan, E., SAR studies of 5-aminopyrazole-4-carboxamide analogues as potent and selective inhibitors of Toxoplasma gondii CDPK1. *ACS Medicinal Chemistry Letters* **2015,** *6* (12), 1184-1189.
22. Arnold, S. L. M.; Choi, R.; Hulverson, M. A.; Schaefer, D. A.; Vinayak, S.; Vidadala, R. S. R.; McCloskey, M. C.; Whitman, G. R.; Huang, W.; Barrett, L. K.; Ojo, K. K.; Fan, E.; Maly, D. J.; Riggs, M. W.; Striepen, B.; Van Voorhis, W. C., Necessity of bumped kinase inhibitor gastrointestinal exposure in treating cryptosporidium infection. *The Journal of Infectious Diseases* **2017,** *216* (1), 55-63.
23. Vidadala, R. S. R.; Rivas, K. L.; Ojo, K. K.; Hulverson, M. A.; Zambriski, J. A.; Bruzual, I.; Schultz, T. L.; Huang, W.; Zhang, Z.; Scheele, S.; DeRocher, A. E.; Choi, R.; Barrett, L. K.; Siddaramaiah, L. K.; Hol, W. G. J.; Fan, E.; Merritt, E. A.; Parsons, M.; Freiberg, G.; Marsh, K.; Kempf, D. J.; Carruthers, V. B.; Isoherranen, N.; Doggett, J. S.; Van Voorhis, W. C.; Maly, D. J., Development of an Orally Available and Central Nervous System (CNS) Penetrant Toxoplasma gondii calcium-dependent protein kinase 1 (TgCDPK1) inhibitor with minimal human ether-a-go-go-related gene (hERG) activity for the treatment of Toxoplasmosis. *Journal of Medicinal Chemistry* **2016,** *59* (13), 6531-6546.

24. Tatipaka, H. B.; Gillespie, J. R.; Chatterjee, A. K.; Norcross, N. R.; Hulverson, M. A.; Ranade, R. M.; Nagendar, P.; Creason, S. A.; McQueen, J.; Duster, N. A.; Nagle, A.; Supek, F.; Molteni, V.; Wenzler, T.; Brun, R.; Glynne, R.; Buckner, F. S.; Gelb, M. H., Substituted 2-Phenylimidazopyridines: A new class of drug leads for human african Trypanosomiasis. *Journal of Medicinal Chemistry* **2014,** *57* (3), 828-835.
25. Vinayak, S.; Pawlowic, M. C.; Sateriale, A.; Brooks, C. F.; Studstill, C. J.; Bar-Peled, Y.; Cipriano, M. J.; Striepen, B., Genetic modification of the diarrheal pathogen Cryptosporidium parvum. *Nature* **2015,** *523* (7561), 477-480.

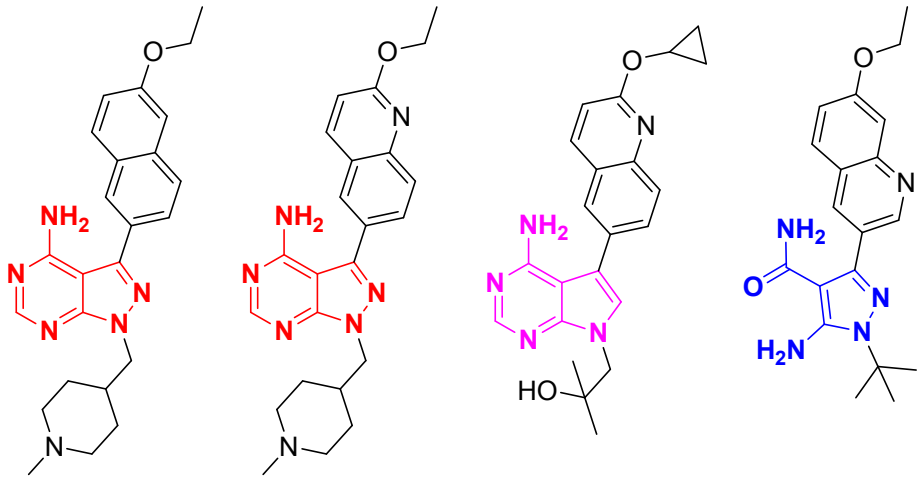

Figure 1. BKI structures that are potent *Cp*CDPK1 inhibitors and effective in the mouse and/or calf models of cryptosporidiosis.

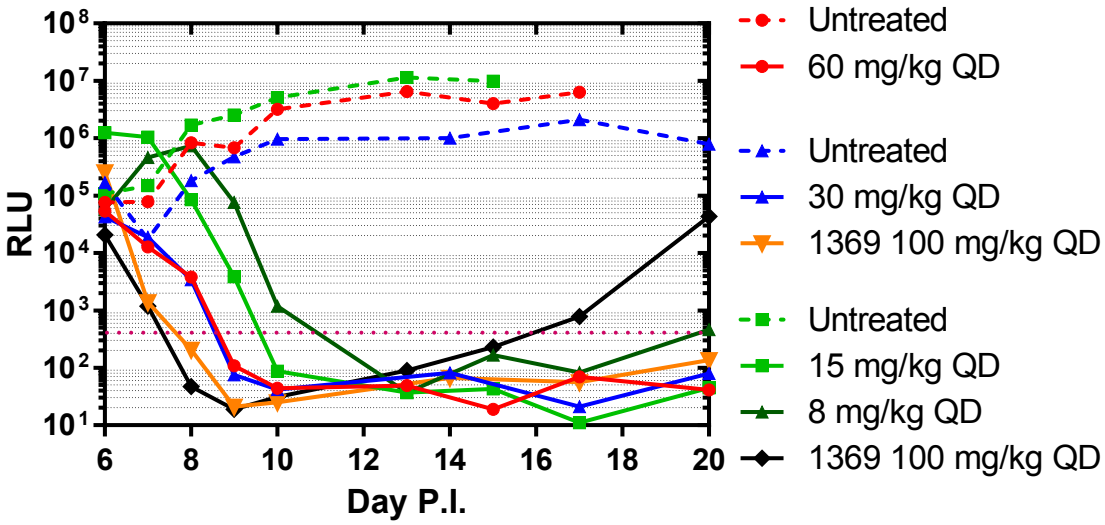

Figure 2A. Compound **6** (1708) IFN-γ KO mouse efficacies. Groups lacking readouts through day 20 were euthanized on their last readout day due to weight loss.

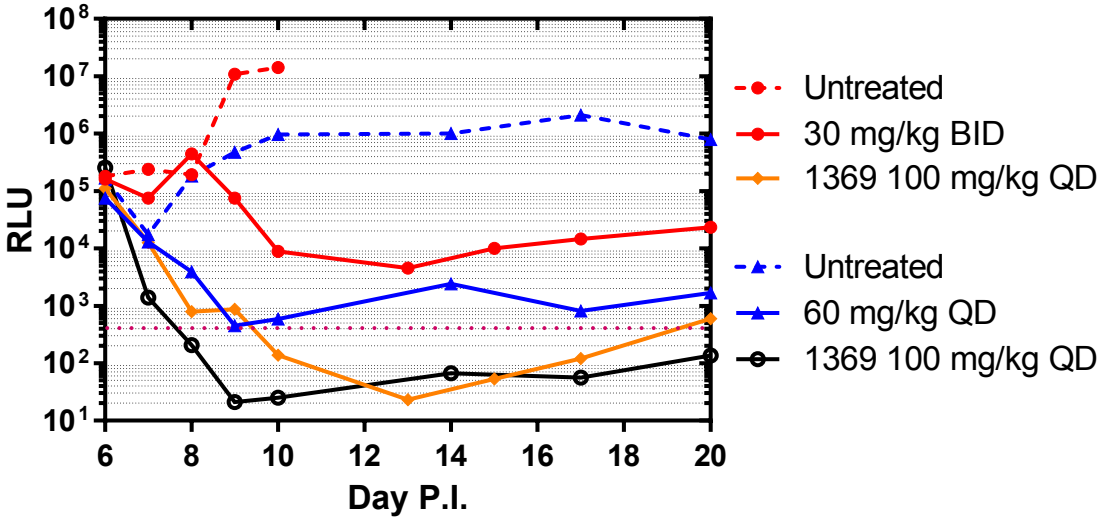

Figure 2B. Compound **9** (1768) IFN-γ KO mouse efficacies. Groups lacking readouts through day 20 were euthanized on their last readout day due to weight loss.

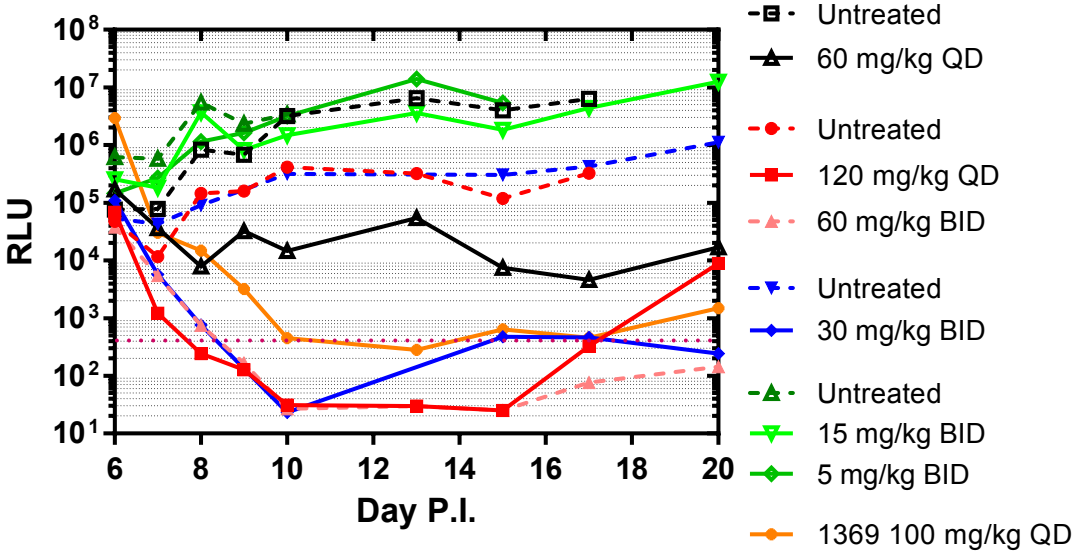

Figure 2C. Compound **15** (1770) IFN-γ KO mouse efficacies. Groups lacking readouts through day 20 were euthanized on their last readout day due to weight loss.

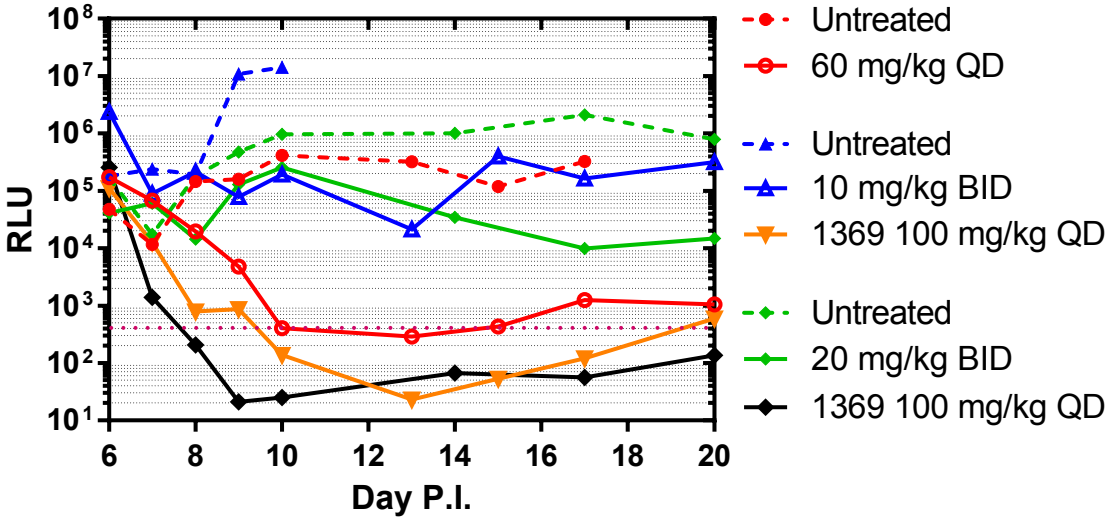

Figure 2D. Compound **20** (1748) IFN-γ KO mouse efficacies. Groups lacking readouts through day 20 were euthanized on their last readout day due to weight loss.

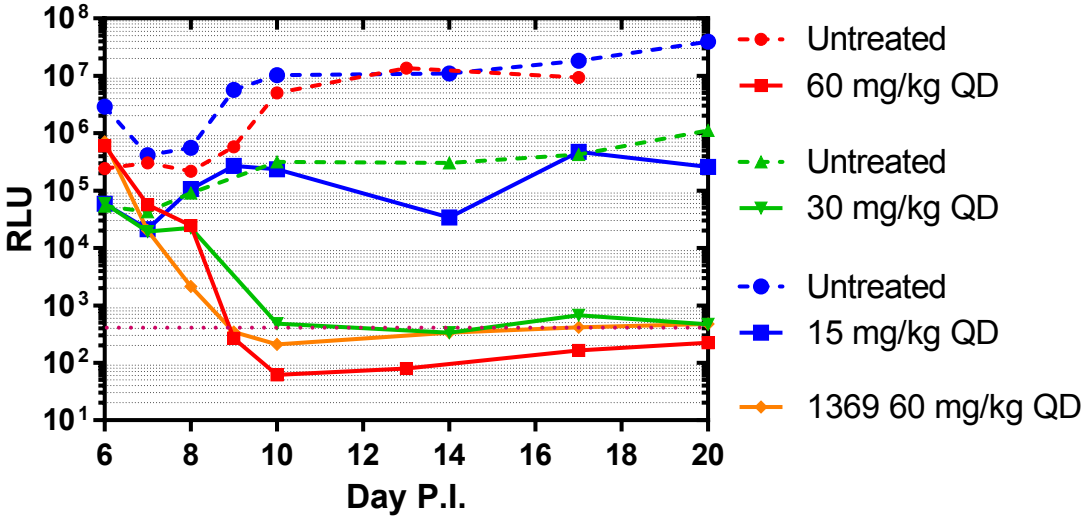

Figure 2E. Compound **25** (1673) IFN-γ KO mouse efficacies. Groups lacking readouts through day 20 were euthanized on their last readout day due to weight loss.

Table 1. AC BKI structures and associated in vitro results

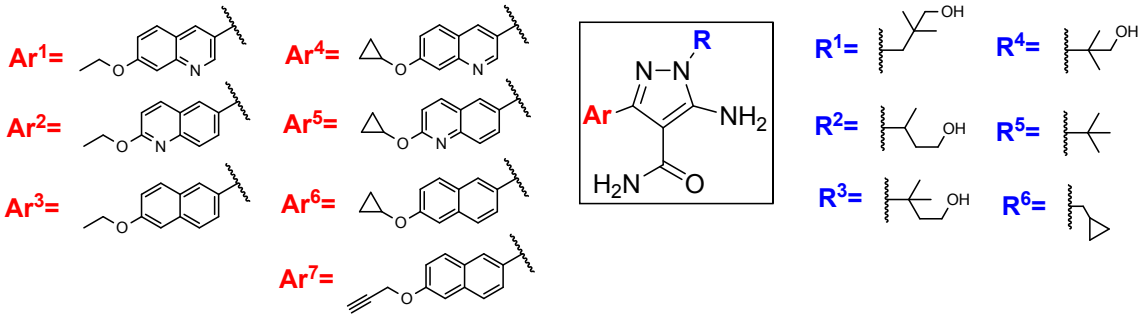

Compd	BKI	Ar/R	*Cp*CDPK1 IC_{50}	*C. parvum* EC_{50}	SRC IC_{50}	hERG (thallium)	hERG (Qpatch)	Protein binding (Mouse)	Protein binding (Human)	Solubility pH 2.0	Solubility pH 6.5
			μM	μM	μM	μM	μM	%	%	μM	μM
1	1596	Ar^1/R^1	0.0047	1.82	>10	>30	*ND*	*ND*	*ND*	*ND*	>100
2	1622	Ar^2/R^1	0.0024	0.89	>10	*ND*	*ND*	*ND*	*ND*	>50	>100
3	1772	Ar^3/R^1	0.0066	0.88	6.3	30	>8.6	92	94	>100	20.6
4	1773	Ar^4/R^1	0.0001	1.22	>10	*ND*	*ND*	*ND*	*ND*	>100	>100
5	1774	Ar^5/R^1	0.0034	0.73	>10	>30	3.2	67	91	>100	100
6	1708	Ar^6/R^1	0.0007	0.41	>10	13	12.3	89	99.9	93	98
7	1608	Ar^1/R^2	0.0055	0.71	3.5	>30	*ND*	86	84	78	>100
8	1711	Ar^2/R^2	0.0046	0.42	5.4	>30	*ND*	*ND*	*ND*	*ND*	*ND*
9	1768	Ar^3/R^2	0.002	0.37	10	>30	*ND*	71	88	>100	56.7
10	1769	Ar^4/R^2	0.002	0.43	>10	>30	*ND*	*ND*	51	>100	>100
11	1712	Ar^5/R^2	0.0059	0.6	>10	>30	*ND*	77	*ND*	>100	98
12	1713	Ar^6/R^2	0.0060	0.45	>10	>30	*ND*	95	95	>100	>100
13	1743	Ar^1/R^3	0.0057	3.3	2.5	>30	*ND*	*ND*	*ND*	87.9	>100
14	1744	Ar^2/R^3	0.0043	0.65	>10	>30	*ND*	*ND*	*ND*	>50	>50
15	1770	Ar^3/R^3	0.0025	0.51	>10	>30	>17.3	94	99	75	60.2
16	1771	Ar^4/R^3	0.003	0.53	>10	>30	*ND*	*ND*	*ND*	88.8	*ND*
17	1745	Ar^5/R^3	0.0023	0.25	>10	30	*ND*	*ND*	*ND*	96	>100
18	1746	Ar^6/R^3	0.0038	0.44	>10	4.5	*ND*	*ND*	*ND*	>100	*ND*
19	1747	Ar^1/R^4	0.0041	0.74	4.7	>30	*ND*	*ND*	*ND*	>50	>50
20	1748	Ar^2/R^4	0.0031	0.21	>10	>30	>21.5	80	84	>100	>100
21	1749	Ar^3/R^4	0.009	0.49	>10	>30	*ND*	91	97	18.8	8
22	1780	Ar^4/R^4	0.0019	1.32	>10	>30	*ND*	*ND*	*ND*	89	44.2
23	1751	Ar^5/R^4	0.0038	0.71	>10	>30	*ND*	85	95	>100	>100
24	1750	Ar^6/R^4	0.0069	0.66	>10	30	>30	80	*ND*	89	92.9
25	1673	Ar^6/R^5	0.0043	0.35	>10	27	>17	95	82	83	65
26	1757	Ar^7/R^5	0.0017	0.71	>10	*ND*	>22.6	88	99	17.6	<10
27	1779	Ar^3/R^6	0.00003	1.03	10	15.7	*ND*	97	95	50.6	7.4

ND=not done

Table 2. Pharmacokinetic values from a single oral dose in mice.

Entry	BKI	Dose (mg/kg)	T_{max} (min)	C_{max} (μM)	AUC (min*μmol/L)	Half Life (min)	Oral Clearance (mL/min)	Fecal concentration from 25 mg/kg dose (μM)
2	1622	10	50	2.4	140.2	6.3	5.1	*ND*
3	1772	25	50	3.1	621.1	206.8	2.1	7.6
5	1774	25	30	1.9	11910	11777.5	0.1	41
6	1708	10	30	2.9	247.1	42.6	2.2	*ND*
7	1608	10	30	2.7	339	119.7	1.9	1.1
9	1768	25	40	10	1738	355	0.8	*ND*
10	1712	25	30	69.2	11769	122.8	0.1	4.5
11	1769	25	40	8.5	1154.1	85.1	0.7	*ND*
12	1713	25	30	15.4	4332.8	134.4	0.3	10.3
14	1744	25	30	2.8	397.4	402.8	3.8	0.5
15	1770	25	30	2.8	144.5	21.1	11.1	2.8
17	1745	25	30	1.6	193.6	69.3	6.7	0.92
18	1746	25	30	6.6	483.2	101.5	1	*ND*
19	1747	25	80	133.2	50798.1	137.6	1	2.9
20	1748	25	70	38.6	11412.6	163.5	0.4	0.41
21	1749	25	90	24	9365	211.2	0.2	7.1
23	1751	25	80	13.8	7913.5	50	0.2	*ND*
24	1750	25	180	79.2	41782	160.2	0.3	3.5
25	1673	10	180	12.9	9098	481.5	0.5	0.42
26	1757	25	160	16.9	11461.9	289.5	0.1	24
27	1779	25	50	4.2	2800.8	758.1	0.5	54

ND=not done

Table 3. Efficacy results from *C. parvum* infected interferon-γ knockout mice.

Compound	Dose (mg/kg)	Log reduction of infection from untreated controls
3	60	-0.03
5	60	4.27
6	60	4.09
7	60	3.41
9	60	2.62
12	60	4.78
15	60*	3.37
20	60	3.15
21	25**	0.81
23	60	4.53
24	60	4.47
25	60	3.52
26	60	0.25
27	25**	0.76

*Dosed twice daily due to short $T_{1/2}$ and fast oral clearance; all other compounds dosed once daily
**Dosed at lower concentration due to mild toxicity in multiple dosing at 60 mg/kg in previous unrelated experiments (data not published)

Table 4. Reasons individual compounds were either removed from consideration or further tested

Compound	BKI	Liabilities
1	1596	Less potent than similar compounds
2	1622	*
3	1772	Failed efficacy, low c-Src IC_{50}
4	1773	Less potent than similar compounds
5	1774	Low hERG- cardiovascular liabilities
6	1708	N/A - moved to dose response
7	1608	Low c-Src IC_{50}
8	1711	Low c-Src IC_{50}
9	1768	N/A - moved to dose response
10	1712	High systemic distribution, similar to 1713
11	1769	*
12	1713	Signs of toxicity during efficacy
13	1743	Low c-Src IC_{50}
14	1744	*
15	1770	N/A - moved to dose response
16	1771	*
17	1745	Low hERG- cardiovascular liabilities
18	1746	Low hERG- cardiovascular liabilities
19	1747	Low c-Src IC_{50}
20	1748	N/A - moved to dose response
21	1749	Failed efficacy
22	1780	Less potent than similar compounds
23	1751	Signs of toxicity during efficacy
24	1750	In vivo cardiovascular liabilities (data not shown)
25	1673	N/A - moved to dose response
26	1757	Failed efficacy
27	1779	Failed efficacy

* Warrant further investigation, but not examined yet due to structural similarities with other compounds

Table 5. Plasma concentrations during multiple dose toxicity in mice.

Compound **6** Plasma Concentration (μM)		
Time Sampled	Dose Concentration	
	100 mg/kg QD	200 mg/kg QD
pre dose 2	1.6 ± 1.9	5.0 ± 2.8
0.5h post dose 2	67.0 ± 23.7	25.9 ± 19.5
1h post dose 2	124.5 ± 56.7	79.1 ± 36.5
pre dose 5	9.6 ± 5.8	3.0 ± 2.2
0.5h post dose 5	35.2 ± 11.1	44.5 ± 11.7
1h post dose 5	139.5 ± 82.1	111.6 ± 29.5

Compound **15** Plasma Concentration (μM)		
Time Sampled	Dose Concentration	
	150 mg/kg QD	300 mg/kg QD
pre dose 2	0	0
0.5h post dose 2	27.8 ± 12.9	30.5 ± 6.1
1h post dose 2	23 ± 13.3	24.6 ± 1.3
pre dose 5	0	0
0.5h post dose 5	30.2 ± 5.7	34.1 ± 8.6
1h post dose 5	24.7 ± 3.2	16.7 ± 5.1

Compound **25** Plasma Concentration (μM)		
Time Sampled	Dose Concentration	
	100 mg/kg QD	250 mg/kg QD
2h post dose 2	36.6 ± 2.7	40.1 ± 1.6
pre dose 3	19.9 ± 5.4	36.1 ± 16.7
2h post dose 5	49.2 ± 4.7	72.2 ± 5.2
24h post dose 7	26.4 ± 15	24.6 ± 3
48h post dose 7	4.8 ± 4.1	2.3 ± 0.4
72h post dose 7	0.3 ± 0.1	0.7 ± 0.3

Table of Contents Graphic

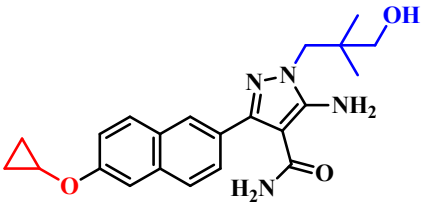

6 (BKI 1708)

Efficatious at 8 mg/kg QD
Safe at > 200 mg/kg
No cardiotoxicity liabilities

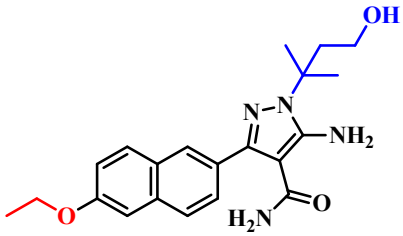

15 (BKI 1770)

Efficatious at 30 mg/kg BID
Safe at > 300 mg/kg
No cardiotoxicity liabilities